# Impact Modelling of Cermet Composites



# Impact Modelling of Cermet Composites

**E Postek[1,*], T Sadowski[2]**

[1] Department of Information and Computational Science, Institute of Fundamental Technological Research Polish Academy of Sciences, Pawinskiego 5B, 02-106 Warsaw, Poland
[2] Department of Solid Mechanics, Lublin University of Technology, Nadbystrzycka 40 str., 20-618 Lublin, Poland

*Corresponding author: epostek@ippt.pan.pl

**Abstract**. The WC/Co is one of broad class of cermet materials (CM) that are applied in fabrication of machining tools. It means that they are subjected to different kind of dynamic loadings. They have very good mechanical properties. However, the degradation of the CM material under dynamic load has not been enough thoroughly investigated. Experimental results yield that the dissipation of the fracture energy in WC/Co samples is due to Co ductile failure at the WC and Co interface [1] and/or dimple rupture mechanism [2]. Stress concentrations about stress raisers such as grain bounds cause microcracking that is further propagated by dynamic loading. However, there are no such predictions for impact conditions. The main goals of the presentation are to explore the formerly created models of the two-phase composite [3, 4] towards impact conditions impacts and give qualitative predictions of the crack and plastic strains initiation for such cases. It has been found that microcracks development process and stress fields depend on impact velocity and the existence of discontinuities: (1) inside the Co binder and (2) the interface between the binder and the grains. Estimation of the microcracks distribution by means of damage parameter is given.

## 1. Introduction

New technological processes very often need up-to-date materials of polycrystalline structure. Ceramic Matrix Composites (CMC) and monolithic ceramics are presented in, for example [1, 2]. Different models of the materials are given in, for example, [3-14]. Further on, nanoceramics is of more complicated structure [15, 16] and the same concerns functionally graded materials [17-21]. The other CMs materials, for example, titanium/molybdenum carbides and tungsten carbide with cobalt binders (WC/Co) are described in [22-28]. Methodologies of assessment the properties of complex materials are presented in [29-36].

Behaviour of novel composites in the context of the multiscale modelling is commonly investigated, [37-40]. For example, two-scale approach that decomposes the case into levels of the respective fine and coarse scale is derived by de Borst [37]. The multiscale modelling encounters the fundamental problem of coupling the different scales taking into account different discretization paradigms, i.e. finite elements, finite differences, meshless methodologies, etc. A variational multiscale approach pretends to be the successful methodology for scales coupling, [39]. The partition-of-unity approach for multiscale models of CM and CMC appear to be successful [37].

CM behaviour due to impact loading is more complex than one phase polycrystalline ceramics. It concerns the modelling of the CMs as well.

For example, the WC/Co properties were examined experimentally, [22, 23, 41]. Concerning our model of impact of CMs, we apply meso-mechanical way of modelling for the RVE containing grains and thin continuous intergranular layers. Experiments on thin metallic intergranular layers in CMs have been described, for instance, in: [22, 23] for WC/Co, [42] for a Pt layer on $Al_2O_3$, [43] for $Al_2O_3$ bonded with pure Al and Al with addition of 4% Mg, [44] for TiC-$Mo_2C$ grains with Ni binder. It has been shown in experiments [43] that metallic interfaces are soft enough that failure mechanism is ductile. Considering [23, 24] we note that in the WC/Co CMs, the most of the fracture energy is dissipated via the ductile failure of the soft Co binder. In the failure, the two fracture mechanisms are engaged, namely, dimple rupture mechanism [64] and microcracks development in the Co binder/ WC grain interface, [65]. Co binder ductile failure seems to be the main mechanism of fracture resistance in the WC/Co CM, [24].

Up to now, the evaluation of equivalent mechanical constants of CMs has been carried out under static load, for example, [33], [44-49]. The loading models depict continuous modifications of the material. The changes of the internal structure concern rotations of grains, peaks of plastic strains in metallic binders, microcracks development [28, 50-51]. In the mentioned papers, the authors investigate ductile failure of the Co intergranular thin layer with I fracture initiation mechanism. It means, the coalescence of micro-voids that further cause cracking nucleation and then their propagation. Description of the II fracture initiation mechanism of the Co binder is given in [23, 24]. The ductile failure of the Co binder is caused by phenomena that initiate in the WC/Co interface. It has been found that the role of the interfaces is important and depending on the phenomena in interfaces may trigger different ways of cracks advancement. For example, the phenomenon has been observed in the CMC bi-material interfaces [52-54]. In this case, the nucleated cracks can be arrested for a moment or can advance along the stiff bound barrier.

WC/Co is widely purchased for fabrication of cutting tools. Therefore, the understanding of the microcracks development that is vital for the durability of the tools is of high importance. The mirocracking process is revealed in experiments for repeatable compressive load [55], and also for repeated impacts [74]. Layered composites under dynamic load are described in [66-68, 76]. Examples of impacts and blasts exerted on such structures are shown, for example, in [67, 69-73, 75]. Nevertheless, we still see a gap in the wide literature concerning WC/Co behaviour in the case of impacts.

To extend previously developed models for the quasi-static loading of the WC/Co [28, 47–51] we analyse microcracks development during compressive impact of the CM sample into rigid wall. It is justified by the fact that short impacts appear during hard materials machining. The numerical model under consideration takes into account dimensions and structure of the components. The constitutive laws are considered for the components, as well. In consequence, the factors that affect internal structure of the CM variation are as follows: (a) positions of CM components, (b) presence of grain/binder transition zones (interfaces) that are the microcracks triggers, (c) finite deformations of the Co intergranular layers (binders), (d) plastic strains in binders, (e) grains rotation. The other vital factor is the velocity of the impact. It was shown by means of damage parameter that has been pointed out peaks of microcracks, [56].

## 2. Physical and numerical model

The CM polycrystal consists of the elastic WC grains of very high strength and Co binders that are elastic-plastic. The constitutive material model is in agreement with experiments that are shown in [24, 43]. While the grains are discretized with hexahedral 3D elements only the binders are discretized with assemblage of 3D hexahedrals and 3D interface elements. The interface elements are present in the binders, in the binders joints and in their structure. They allowed introducing discontinuities into the model.

The finite element model stands for the Representative Volume Element (RVE) of the CM. The calculation scheme of the system that includes CM sample, rigid wall and initial and boundary

conditions is shown in figure 1. The sample impacts the rigid wall along *x*-axis of the model. The individual discretizations of the binders and the grains are presented in figure 2 and figure 3.

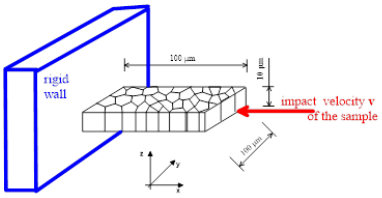


**Figure 1**. Scheme of the structure.

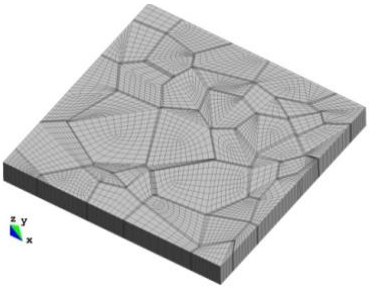

**Figure 2**. Discretization of the sample.

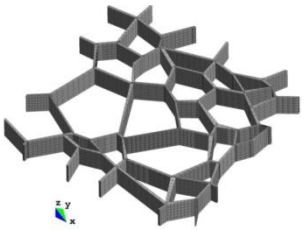

**Figure 3.** Discretization of the interfaces.

We consider two models, continuous (M1) and discontinuous (M2). The potential discontinuities are allowed by the interface elements that are inserted into the binders. The model M1 counts 34572 linear C3D8 hexahedrals and 41216 nodal points. The model M2 is additionally enriched with 47407 linear 8-nodes interface elements that cause the increase of the number of nodal points up to 152169. We apply MSC Patran [58] for geometrical modelling, Abaqus program for the numerical simulations [57] and program GiD for the postprocessing phase [59]. The material properties of the grains read: Young's modulus is $4.1\text{x}10^{11}$ Pa, and Poisson's ratio is 0.25. The intergranular binders are elastic-plastic with Young's modulus $2.1\text{x}10^{11}$ Pa, Poison's ratio 0.235, yield stress $2.97\text{x}10^{8}$ Pa. The material obey the isotropic hardening rule.

The created finite element model allows for the brick elements separation in the cobalt binders. It is achieved by the inserting of the cohesive interface elements that surrounds each of the hexahedral element in the binder. The properties of the binders are established considering the work [26], and adopting the traction-separation constitutive law in the interface elements, [60, 61].

The constitutive parameters of the constitutive law in the interfaces read: elastic modulus normal to the midsurface of the interface element (*n*) is $2.1\text{x}10^{11}$ Pa, both shear moduli in the directions that are tangent to the midsurface of the interface element (*s, t*) read $1.373\text{x}10^{11}$ Pa. The damage initiation condition is postulated quadratic:

$$\left\{\frac{\varepsilon_n}{\varepsilon_n^o}\right\}^2+\left\{\frac{\varepsilon_s}{\varepsilon_s^o}\right\}^2+\left\{\frac{\varepsilon_t}{\varepsilon_t^o}\right\}^2=1 \tag{1}$$

In the equation above, $\varepsilon_n$ is the nominal strain in the normal direction *(n)* to the midsurface of the interface element, and $\varepsilon_s$, $\varepsilon_t$ are the nominal strains in the two orthogonal *(s)* and *(t)* tangent directions to the midsurface of the interface element. The variables $\varepsilon_n^o$, $\varepsilon_s^o$, $\varepsilon_t^s$ are the maximum nominal strains at the normal mode (*n*) and the shear modes in the directions (*s*) and (*t*) with the postulate of their independence. The maximum nominal strains are $2.5\text{x}10^{-4}$, $6.65\text{x}10^{-4}$ and $6.65\text{x}10^{-4}$, respectively. Considering the isotropic damage, the maximum reduced stress is given as follows, [62]:

$$\sigma_{\max}^D=\sigma_{\max}(1-D) \tag{2}$$

The reduced stress refers to the damage variable $D=A/A_o$ with the damaged cross-section area *A,* and the area of the pristine cross-section $A_o$. The damage variable *D* is in the range of 0 and 1. The D

variable The evolution of the damage variable follows an exponential rule. The damage variable reflects the deterioration of the cross-section because of microcracks showing up in the course of loading path. The evolution equation of damage variable is as follows, [60]:

$$D = 1 - \left( \frac{\delta_m^o}{\delta_m^{\max}} \right) \left( 1 - \frac{1 - \exp\left( -\alpha \left( \frac{\delta_m^{\max} - \delta_m^o}{\delta_m^f - \delta_m^o} \right) \right)}{1 - \exp(-\alpha)} \right) \tag{3}$$

The $\sigma_{\max}$ is the stress referred to the cross-section that is not damaged. The stress $\sigma_{\max}^D$ is the stress referred to the pristine cross-section. It is the nominal stress. Further on, $\delta_m^o$ is the displacement at which the stress touches the maximum strength $\sigma_{\max}$ at the start of damage, $\delta_m^{\max}$ is the maximum displacement attained in the loading path, $\delta_m^f$ is the failure displacement, and $\alpha$ is the damage rate.

## 3. Numerical results

We note qualitative dissimilarity in displacement fields in the models M1 and M2 that undergo the impact velocity of 50 m/s. While comparing figure 4(a) and figure 4(b) we observe significant influence of the discontinuities in the binders. We mind a wedge that builds along the grains bounds, figure 4(a). Another observation concerns the displacement fields, namely, we find that the displacement field in the case M1 is smoother than in the case of model M2, figure 4(b).

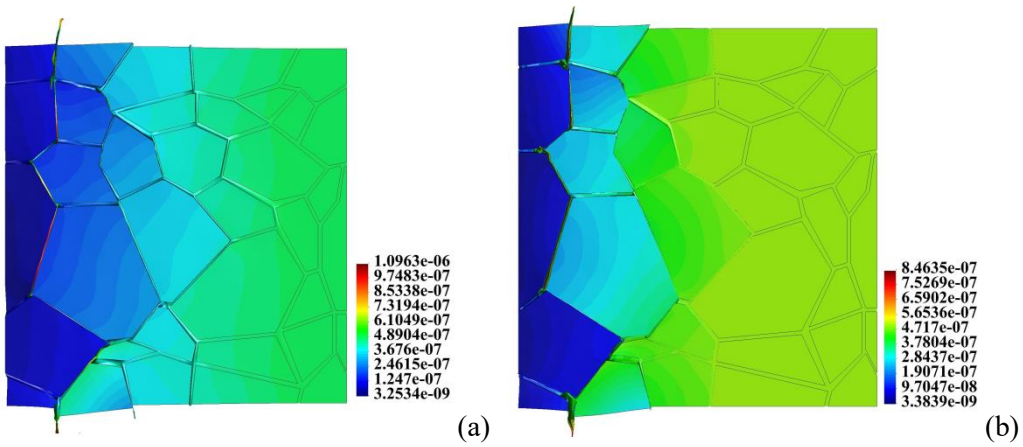


**Figure 4.** Displacement fields for two models, top view: (a) case M1; (b) case M2.

In contrast to model M1, the wedge is not formed in case M2. In both cases we can see thinning of the binders and squeezing their material off. However, we note that the squeezing off of the interfaces material in case M1 is more intense than in the case M2. In model M2, the discontinuities are sharper than in case of M2. In cases M1 and M2, the maximum displacements are 1.10E-06 m and 8.46E-07 m with the difference 23.1%. The squeezing off develops along the formed wedge, figure 5(a) and ranges deeper into the sample than in case of model M2, figure 5(b). The squeezed-out material is more distributed in the model with discontinuities.

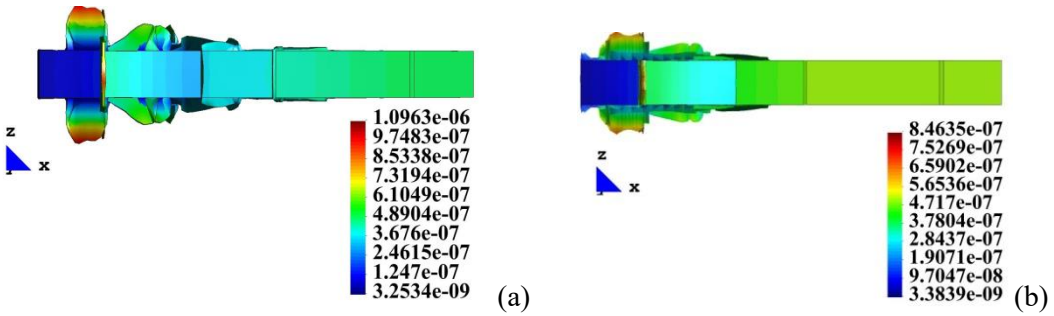


**Figure 5.** Displacement fields for two models, side view: (a) case M1; (b) case M2.

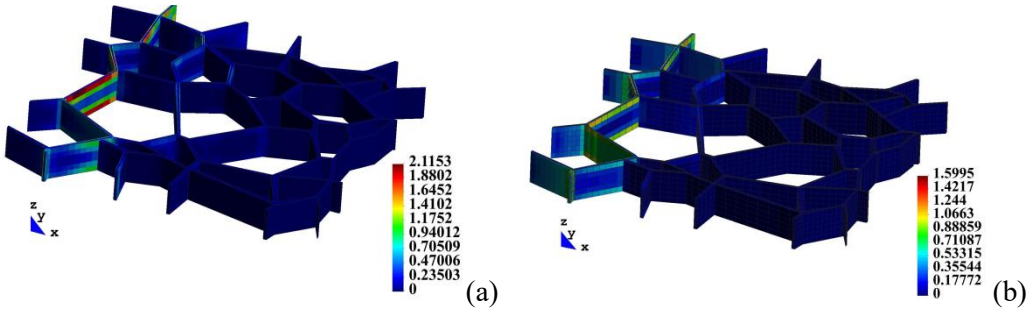


**Figure 6.** Equivalent plastic strain distribution in binders, time instant 1.0E-08 s: (a) case M1; (b) case M2.

Gross equivalent plastic strain is qualitatively similarly distributed in binders in both models, figure 6. However, the plastic deformation is higher in case M1 than in case M2 with the difference of 134%. We note that plastic strains in interfaces start to develop mostly at the edges of the interfaces. It concerns both M1 and M2 models. The effect can be seen particularly well in the binders that are placed close to the striking edge of the sample.

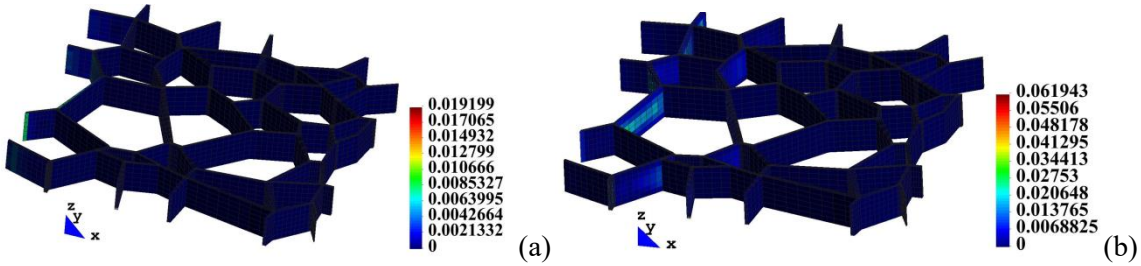


**Figure 7.** Damage parameter development: (a) time instant 2.0E-09 s; (b) time instant 1.0E-08 s.

The damage parameter distribution is given in figure 7. Damage appears in interfaces at the attacking edge, figure 7 (a). When the process advances, damage propagates into the interfaces system. We note that damage is higher in the middle of interfaces than at their edges, figure 7(b). We recall here figure 6 that illustrates spatial distribution of plastic strains. We note a qualitative difference between damage parameter distribution and equivalent plastic strain distribution. Plastic strains have appeared on the edges of interfaces while damage parameter is high inside interfaces.

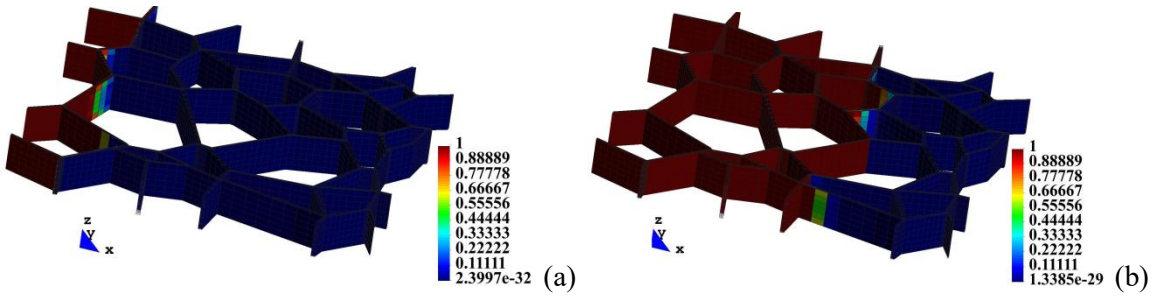


**Figure 8.** Microcracks development: (a) time instant 2.0E-09 s; (b) time instant 1.0E-09 s.

We follow the microcracking process in figure 8. This is done for model M2. We find that the cracking process advances uniformly into the interfaces system. The front of the cracked interfaces is practically parallel to the attacking edge of the sample.

## 4. Final remarks

We point out main attributes of the new model and the summary of our observations that are as follows:

- the model suits well for loading due to impact,
- since the displacement fields and thereafter the shapes of the sample, and values of the other variables, are dissimilar when analyzing the continuous and discontinuous models, the model that includes the cracks effect should be considered,
- in the continuous model, the grains move and create a visible wedge,
- concerning the discontinuous model the grains do not build the wedge but they move along the binders that are about parallel to the striking boundary of the sample,
- plastic strains and damage parameter give their presence at the start of the impact process,
- plastic strains shows up in the bounds of binders and develop towards their interior,
- damage parameter starts to grow in the interior of the interfaces.

The model is intended to develop RVE [63, 77] of larger size and more precise.

**Acknowledgments**

This work was financially supported by Ministry of Science and Higher Education (Poland) within the statutory research (IPPT PAN) and National Science Centre (Poland) project No 2016/21/B/ST8/01027 (Lublin University of Technology). The calculations were done at the Interdisciplinary Centre for Mathematical and Computational Modelling, University of Warsaw, Poland. The licenses for the MSC Patran and Abaqus programs were provided by Academic Computer Centre in Gdańsk, Poland.

**References**

[1] Fett T and Munz D 1999 *Mechanical Properties, Failure Behaviour, Materials Selection, Ceramics* (Berlin Heidelberg New York: Springer)
[2] Rice R W 1998 *Porosity of ceramics* (New York: Marcel Dekker Inc.)
[3] Gömze L A and Gömze L N 2009 *Építöanyag: JSBCM* **61** 38-42
[4] Sadowski T and Samborski S 2003 *J. Am. Cer. Soc.* **86** 2218-21
[5] Gömze L A and Gömze L N *IOP Conf. Ser.: Mater. Sci. Eng*. **47** 012033
[6] Sadowski T and Samborski S 2003 *Comp. Mat. Sci*. **28** 512-17
[7] Espinoza H D and Zavattieri P D 2003 *Mech. Mater.* **35** 333-64
[8] Espinoza H D and Zavattieri P D 2003 , *Mech. Mater.* **35** 365-94
[9] Sadowski T and Marsavina L 2011 *Comput. Mat. Sci.* **50** 1336-46
[10] Sadowski T 2012 *Comput. Mat. Sci.* **64** 209-11

[11] Sadowski T and Samborski S 2008 *Comp. Mater. Sci*. **43** 75-81
[12] Ghosh D, Banda M, Akurati S, Kang H and Fakharizadeh O 2017 *Scripta Mater.* **138** 139-44
[13] Sadowski T and Pankowski B 2016 *Comp. Struct.* **143** 388-94
[14] Sadowski T and Golewski G 2008 *Comp. Mat. Sci.* **43** 119-26
[15] Winter M 2002 *Nanocrystalline ceramics, synthesis and structure* (Berlin: Springer)
[16] Koch C C, Ovid'ko I A, Seal S and Veprek S 2007 *Structural nanocrystalline materials: fundamentals and applications* (Cambridge: Cambridge Univ. Press)
[17] Suresh S and Mortensen A 1998 *Fundamentals of functionally graded materials* (Cambridge: The University Press)
[18] Sadowski T, Marsavina L, Peride N, Craciun E M 2009 *Comput. Mat. Sci.* **46** 687-693
[19] Marsavina L, Linul E, Voiconi T, Sadowski T 2013 *Polymer Testing* **32** 673-680
[20] Sadowski T and Golewski P 2012 *Comput. Mat. Sci.* **52** 293-97
[21] Sadowski T and Golewski P 2012 *Comput. Mat. Sci.* **64** 285-88
[22] Siegl L S and Exner H E 1987 *Metall. Trans. A.* **18A** 1299-308
[23] Siegl L S and Fischmeister H F 1988 *Acta Metall.* **136** 887-97
[24] Ravichandran K S 1994, *Acta Metal. Mater.* **42** 143–50
[25] Hönle S and Schmauder S 1998 *Comput. Mater. Sci.* **13** 56-60
[26] Felten F, Schneider G and Sadowski T 2008 *Int. J. Ref. Mat. Hard. Mat.* **26** 55-60
[27] Li W, Wang H, Wang L, Hou C, Song X, Liu X and Han X 2017 *Mat. Res. Letters* **5** 55-60
[28] Postek E and Sadowski T 2011 *Comp. Interf.* **18** 57-76
[29] Nemat-Nasser S and Horii M 1999 *Micromechanics: overall properties of the heterogeneous materials* (Amsterdam – New York – Oxford – Tokyo: Elsevier)
[30] Kachanov M 1993 *Advances in Appl. Mech*. **30** 259-445
[31] Gross D andSeelig T 2006 *Fracture mechanics with an introduction to micromechanics*, (Berlin- Heidelberg: Springer)
[32] de Borst R and Sadowski T (Eds) 2008 *Lecture notes on composite materials* (Wien-New York: Springer)
[33] Schmauder S and Mishnayevsky L *Micromechanical and nanosimulation of metals and composites* (Berlin Heidelberg: Springer)
[34] Sadowski T and Trovalusci P (Eds) 2014 *Multiscale Modelling of of Complex Materials, CISM Courses and Lectures No. 556 International Centre for Mechanical Sciences* (Wien – NewYork: Springer)
[35] Altenbach H and Sadowski T (Eds) 2015 *Failure and Damage Analysis of Advanced Materials, CISM Courses and Lectures No. 560 International Centre for Mechanical Sciences* (Wien – NewYork: Springer)
[36] Flavata A, Trovalusci P and Masiani R 2016 *Comput. Mater. Sci.* **116** 22-31
[37] de Borst R 2008 *Comput. Mater. Sci.* **43** 1-15
[38] Kassner M L, Nemat-Nasser S, Suo Z, Bao G, Barbour J C, Brinson L C, Espinosa H, Gao H, Granick S, Gumbsh P, Kim K S, Knauss W, Kubin L, Langer J, Larson B C, Mahadevan L, Majumdar A, Torquato S and van Swol F 2005 *Mech. Mat.* **37** 231-59
[39] Hughes T J R 1995 *Comput. Meth. Appl. Mech. Eng.* **127** 387-401
[40] Lippmann N, Steinkopff T, Schmauder S and Gumbsh P 1997 *Comput. Mater. Sci.* **9** 28-35
[41] Soppa E, Schmauder S, Fisher G, Brollo J and Weber U 2003 *Comput. Mat. Sci.* **28** 574-86.
[42] Dalgleish B J, Lu M C and Evans A G 1998 *Acta Metall.* **36** 2029-35
[43] Dalgleish B J, Trumble K P and Evans A G 1989 *Acta Metall.* **37** 1923-31
[44] Zarikson J, Larsson A and Andren H O 2001 *Micron.* **32** 707-12
[45] Sadowski T and Nowicki T 2008 *Comput. Mat. Sci*. **43** 235-41
[46] Tkalich D, Cailletauld G, Yestrebov V Y and Kane A 2017 *Mech. Mater.* **105** 166-87
[47] Sadowski T, Hardy S and Postek E 2005 *Comput. Mat. Sci.* **34** 46-63
[48] Sadowski T, Hardy S and Postek E 2006 *Mat. Sci. Eng. A*. **424** 230-38
[49] Sadowski T, Postek E and Denis C 2007 *Comput. Mat. Sci.* **39** 230-236.

[50] Dębski H and Sadowski T 2014 *Comput. Mat. Sci.* **83** 403-11
[51] Dębski H and Sadowski T 2017 *Comp. Struct.* **159** 121-27
[52] Marsavina L and Sadowski T 2009 *Comput. Mat. Sci.* **45** 693-97
[53] Marsavina L and Sadowski T 2009 *Comput. Mat. Sci.* **44** 941-50
[54] Golewski G, Sadowski T 2014 *Const. Build. Mat.* **51** 207-14
[55] Krüger L, Mandel K, Krause R and Radajewski M 2015 *Int. J. Refrac. Met. Hard. Mat.* **51** 324–31
[56] Zhang H, Lu Q, Zhang L and Fang Z Z 2010 *Int. J. Refr. Met. Hard. Mat*. **28** 434-40
[57] Abaqus 6.13. User's Manual.
[58] http://www.mscsoftware.com/product/patran (accessed 20 December 2017)
[59] http://www.gidhome.com/ (accessed 20 December 2017)
[60] Camanhi P P and Davila C G 2002 *Mixed-Mode Decohesion Finite Elements for the Simulation of Delamination in Composite Materials* NASA/TM-2002-211737
[61] Zavattieri P B, Hector L G and Bower A F 2008 *Eng. Fract. Mech.* **75** 4309-32
[62] Kachanov L M 1986 *Introduction to Continuum Damage Mechanics* (Dordrecht: Martinun Nijhoff Publishers)
[63] Jimenez-Pique E, Turon-Vinas M, Chen H, Trofinov T, Fair J, Tarres E and Llanes L 2017 *Int. J. Refr. Met. Hard. Mat.* **67** 9-17
[64] Liu X, Wang H, Wang L, Hou Ch, Song X, Liu X and Han X 2017 In situ study of fracture behavior of ultrafine WC–Co cemented carbide, *Mater. Res. Lett.* **5** 55-60
[65] Sigl L S and Exner H E 1987 *Metall. Trans. A*. **18** (1987) 1299-308
[66] Kärger L, Baaran J, Gunnion A and Thomson R, 2009 *Compos. Part B*. **40** 71-6
[67] Vo T P, Guan Z W, Cantwell W J and Schleyer G K 2013 *Compos. Part B*. **44** 141-51
[68] El Sayed S and Sridharan S 2001 *Compos. Part B.* **32** 545-53
[69] Krishnan K, Sockalingam S, Bansal S and Rajan S D 2010 *Compos. Part B*, **41** 583-93
[70] Corbett G G, Reid S R and Johnson W 1996 *Int. J. Impact Eng.* **18** 141-230
[71] Grady D 1999 *Int. J. Impact Eng.* **23** 307-17
[72] Kawai N, Tsusru K, Shind D, Motoyashiki Y and Sato E 2011 *Int. J. Impact Eng.* **38** 542-45
[73] Compton B G and Zok F W 2013 *Int. J. Impact Eng.* **62** 75-87
[74] Huang Z Q and Gang L 2017 *Eng. Fail. Anal.* **80** 273-77
[75] Allix O 2001 *Compos. Sci. and Tech.* **61** 2193-205
[76] Guinard S, Allix O, Guédra-Degeorges D and Vinet A 2002 *Compos. Sci. and Tech*. **62** 585-89
[77] Karamnejad A and Sluys L J 2014 *Comp. Meth. Appl. Mech. Eng.* **278** 423-44